

<https://doi.org/10.15407/ujpe67.9.695>

I.A. OBAID,<sup>1</sup> H.K. MOHAMAD,<sup>2</sup> SH.D. AL-SAEEDI<sup>1</sup>

<sup>1</sup> Department of Physics, College of Science, University of Thi-Qar

(Nassiriya 640001, Iraq; [inte.abdullhussein@sci.utq.edu.iq](mailto:inte.abdullhussein@sci.utq.edu.iq), [shakirdiwan\\_2phy@sci.utq.edu.iq](mailto:shakirdiwan_2phy@sci.utq.edu.iq))

<sup>2</sup> College of Science, Al Muthanna University

(Samawah550, Iraq; e-mail: [hadey.mohamad@mu.edu.iq](mailto:hadey.mohamad@mu.edu.iq); [hadeyk2002@yahoo.com](mailto:hadeyk2002@yahoo.com))

## FERRIMAGNETIC CHARACTERISTICS AND SPIN COMPENSATION TEMPERATURES IN THE BLUME–CAPEL MODEL WITH MIXED SPIN-3 AND SPIN-5/2

---

*We study the molecular mean-field theory (MMFT) based on the Gibbs–Bogolyubov free energy function of a ferrimagnetic with mixed spin-3 and spin-5/2 for various magnetic crystal fields in the Blume–Capel model. We have evaluated the free energy depending on the trial Hamiltonian operator. By minimizing the free energy of the present system, we have obtained the characteristic features of the longitudinal magnetizations, compensation temperatures, and re-entrant behaviors in the ranges of low temperatures. In particular, we study the effect of magnetic anisotropies on the critical phenomena for the proposed model. The sublattice magnetization dependence of the free energy function has been discussed as well. Our results predict the existence of multiple spin compensation points in the disordered Blume–Capel system for a square lattice.*

*Keywords:* mixed spin Blume–Capel model, magnetic crystal field, phase transitions, re-entrant behavior, spin compensation temperature.

### 1. Introduction

The researches in the ferrimagnetic materials are normally focused on their importance in technical applications and may be accessible for using information storage devices, microwave communications, microelectronics, and magneto-optical recording systems [1–4]. Because of the increasing demands being placed on the performance of magnetic solids, we observe the high interest in the search for magnetic properties of molecule-based magnets [5–8]. The crystalline nonmetallic (or intermetallic) compounds with  $A_p B_{1-p}$ , where  $A$  and  $B$  are different magnetic atoms, are ferrimagnets due to a strong negative  $A - B$  exchange interaction,

and have been the object of a great deal of research [9]. Neutron diffraction studies of the ternary germanide  $\text{TbMn}_6\text{Ge}_6$  of  $\text{HfFe}_6\text{Ge}_6$ -type structure (Fig. 1) showed that both rare earth and manganese sublattices are present simultaneously at room temperature. However, it has been noticed that, in rare earths of the paramagnets, the  $R\text{-Mn}$  ( $R \equiv \text{Tb-Er}$ ) couplings are large enough depending on the reoccurrence and align the manganese moments of the  $\text{Mn-R-Mn}$  slabs. This gives the ferromagnetic assemblies of  $\text{Nd-}$  and  $\text{SmMn}_6\text{Ge}_6$  and the ferrimagnetic prearrangement detected in  $\text{RMn}_6\text{Sn}_6$  compounds at room temperature [10, 11]. In other words, the ferrimagnetic materials are made up of inequivalent moments that interact antiferromagnetically to produce zero spontaneous magnetization sooner than the Curie point.

---

© I.A. OBAID, H.K. MOHAMAD,  
SH.D. AL-SAEEDI, 2022

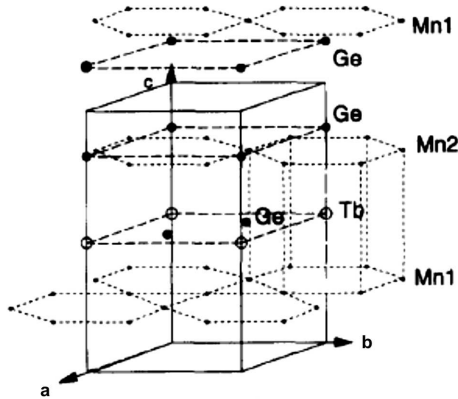


Fig. 1. HfFe<sub>6</sub>Ge<sub>6</sub>-type structure

Thus, a ferrimagnetic behavior at high temperatures in Tb has to be related to a dominant negative Tb–Mn exchange interaction. The authors observed the magnetic behavior which can be described as “bootstrap ferrimagnetism”. At high temperatures, these composites visibly act as archetypal ferrimagnets. However, the bootstrap mechanism linked to the unit cell volume variation yields an antiferromagnetic behavior at low temperatures. C.A. Mercado *et al.* presented a ground-state phase diagram of a mixed Ising model of spins (2, 5/2) on a square lattice. The researchers, in this respect, found a bigger complexity in the phase diagrams due to an increase in the number of interactions and the influence of anisotropy, exploring regions, where important ferrimagnetic behaviors could arise [12]. Furthermore, M. Karimou *et al.* investigated the crystal field and external magnetic field effects on the magnetization of the mixed-spin (7/2, 5/2) ferrimagnetic system by the Monte Carlo simulation and mean-field calculations, respectively. The authors, for specific values of the physical parameters, obtained the compensation temperatures, where the global magnetization vanishes. Particularly, a bilayer magnetic film with an ordered Ising-type Hamiltonian was examined with regard for an interlayer antiferromagnetic coupling [13]. Theoretically, in this work, a point view was reported regarding the extension of efforts to a mixed spin model with one component having spin-3 and another one having spin-5/2. Ground-state phase diagrams are interested to check the reliability of numerical results. For such diagrams at low or high temperatures, some regions induce important magnetic phenomena [14–28]. The aim of this paper is to construct

the ground-state phase structure and to examine the sublattice magnetizations of the disordered alloy under the influence of the crystal fields, within molecular mean-field approximation (MMFA). A Landau–Bogoliubov expression of the free energy in the order parameter is required in this correspondence. This research focus has been directed to the mixed spin system having spin-3 and spin-5/2 with a crystal field interaction. Our work is designed to produce the spin compensation behavior and the re-entrant phenomenon as well.

## 2. Model and Formulation

We will treat the nearest neighbor Blume–Capel Ising model in zero field on a lattice containing two sublattices  $A, B$  having  $N$  sites, each site having  $z$  nearest neighbors. The exchange interaction between  $A$  and  $B$  atoms is assumed an antiferromagnetic. In other words, an antiferromagnetic interaction exists between every nearest-neighbor pair of atoms. So, the proposed work is formulated in terms of the Hamiltonian operator as [16, 17],

$$H = - \sum_{i,j} J_{ij} \lambda_i^A \lambda_j^B - D_A \sum_i (\lambda_i^A)^2 - D_B \sum_j (\lambda_j^B)^2, \quad (1)$$

where the sites of sublattice  $A$  are occupied by spins  $\lambda_i^A$  including the values  $\pm 3, \pm 2, \pm 1, 0$ , and the sites of sublattice  $B$  are occupied by spins  $\lambda_j^B$  with the values of  $\pm 1/2, \pm 3/2, \pm 5/2$ .  $D_A/|J|$ , and  $D_B/|J|$ , are the crystal fields, i.e., magnetic anisotropies acting on the spin-3, spin-5/2, respectively;  $J_{ij}$  is the exchange interaction between spins at sites  $i$  and  $j$ . A systematic way of evaluating the MFM for a microscopic Hamiltonian is to start from the Bogoliubov inequality as [25],

$$f \leq f_0 + \langle H - H_0 \rangle_0, \quad (2)$$

where  $f$  is the approximated free energy,  $H_0$  is a trial Hamiltonian operator depending on variational parameters, and  $f_0$  the corresponding free energy function. In this paper, we consider the suitable choices of a trial Hamiltonian operator, namely,

$$H_0 = - \sum_i [K_A \lambda_i^A + D_A (\lambda_i^A)^2] - \sum_j [K_B \lambda_j^B + D_B (\lambda_j^B)^2], \quad (3)$$

where  $K_A$  and  $K_B$  are the two variational parameters related to the two different spins, respectively. One can evaluate the free energy of the system, i.e., Eq. (2) becomes

$$f = -\frac{1}{2\beta} \left\{ \ln[2e^{9\beta D_A} \cosh(3\beta K_A) + 2e^{4\beta D_A} \times \cosh(2\beta K_A) + 2e^{\beta D_A} \cosh(\beta K_A) + 1] + \ln \left[ 2e^{25/4\beta D_B} \cosh\left(\frac{5}{2}\beta K_B\right) + 2e^{9/4\beta D_B} \times \cosh\left(\frac{3}{2}\beta K_B\right) + 2e^{1/4\beta D_B} \cosh\left(\frac{1}{2}\beta K_B\right) \right] \right\} + 1/2(-zJm_A m_B + K_A m_A + K_B m_B). \quad (4)$$

Minimizing this expression with respect to  $K_A$  and  $K_B$ , one may get self-consistent formulae for the mean magnetic moments (i.e., the reduced magnetizations). They read

$$m_A \equiv \langle \lambda_i^A \rangle_0 = \frac{1}{2} (6 \sinh(3\beta K_A) + 4e^{-5\beta D_A} \times \sinh(2\beta K_A) + 2e^{-8\beta D_A} \sinh(\beta K_A)) / (\cosh(3\beta K_A) + e^{-5\beta D_A} \cosh(2\beta K_A) + e^{-8\beta D_A} \times \cosh(\beta K_A) + 0.5e^{-9\beta D_A}), \quad (5)$$

$$m_B \equiv \langle \lambda_j^B \rangle_0 = \frac{1}{2} \left( 5 \sinh\left(\frac{5}{2}\beta K_B\right) + 3e^{-4\beta D_B} \times \sinh\left(\frac{3}{2}\beta K_B\right) + e^{-6\beta D_B} \sinh\left(\frac{1}{2}\beta K_B\right) \right) / \left( \cosh\left(\frac{5}{2}\beta K_B\right) + e^{-4\beta D_B} \cosh\left(\frac{3}{2}\beta K_B\right) + e^{-6\beta D_B} \cosh\left(\frac{1}{2}\beta K_B\right) \right), \quad (6)$$

where  $\beta = \frac{1}{k_B T}$ , and

$$K_A = zJm_B, \quad K_B = zJm_A. \quad (7)$$

Theoretical studies of mixed Blume–Capel Ising systems have been intensively investigated and show the ferrimagnetic behavior. Then, the spin compensation behavior of the considered system can be obtained by requiring the total magnetization as being equal to zero for various values of crystal fields; though the reduced magnetizations of the proposed model are not equal to zero [23–28], i.e.,

$$M = \frac{1}{2}(m_A + m_B). \quad (8)$$

### 3. Results and Discussion

#### 3.1. Construction of ground-state phase diagram

The mixed spin-3 and spin-5/2 Blume–Capel Ising model exposes twelve phases with various values of  $\{m_A, m_B, \gamma_A, \gamma_B\}$ , i.e., the ordered ferrimagnetic phases:

$$O_1 \equiv \left\{ -3, \frac{5}{2}, 9, \frac{25}{4} \right\} \quad \text{or} \quad O_1 \equiv \left\{ 3, -\frac{5}{2}, 9, \frac{25}{4} \right\},$$

$$O_2 \equiv \left\{ -2, \frac{5}{2}, 4, \frac{25}{4} \right\} \quad \text{or} \quad O_2 \equiv \left\{ 2, -\frac{5}{2}, 4, \frac{25}{4} \right\},$$

$$O_3 \equiv \left\{ -1, \frac{5}{2}, 1, \frac{25}{4} \right\} \quad \text{or} \quad O_3 \equiv \left\{ 1, -\frac{5}{2}, 1, \frac{25}{4} \right\},$$

$$O_4 \equiv \left\{ -3, \frac{3}{2}, 9, \frac{9}{4} \right\} \quad \text{or} \quad O_4 \equiv \left\{ 3, -\frac{3}{2}, 9, \frac{9}{4} \right\},$$

$$O_5 \equiv \left\{ -2, \frac{3}{2}, 4, \frac{9}{4} \right\} \quad \text{or} \quad O_5 \equiv \left\{ 2, -\frac{3}{2}, 4, \frac{9}{4} \right\},$$

$$O_6 \equiv \left\{ -1, \frac{3}{2}, 1, \frac{9}{4} \right\} \quad \text{or} \quad O_6 \equiv \left\{ 1, -\frac{3}{2}, 1, \frac{9}{4} \right\},$$

$$O_7 \equiv \left\{ -3, \frac{1}{2}, 9, \frac{1}{4} \right\} \quad \text{or} \quad O_7 \equiv \left\{ 3, -\frac{1}{2}, 9, \frac{1}{4} \right\},$$

$$O_8 \equiv \left\{ -2, \frac{1}{2}, 4, \frac{1}{4} \right\} \quad \text{or} \quad O_8 \equiv \left\{ 2, -\frac{1}{2}, 4, \frac{1}{4} \right\},$$

$$O_9 \equiv \left\{ -1, \frac{1}{2}, 1, \frac{1}{4} \right\} \quad \text{or} \quad O_9 \equiv \left\{ 1, -\frac{1}{2}, 1, \frac{1}{4} \right\},$$

and disordered phases are defined as  $D_1 \equiv \{0, 0, 0, \frac{25}{4}\}$ ,  $D_2 \equiv \{0, 0, 0, \frac{9}{4}\}$ ,  $D_3 \equiv \{0, 0, 0, \frac{1}{4}\}$ , and the parameters  $\gamma_A$  and  $\gamma_B$  are:

$$\gamma_A = \langle (\lambda_i^A)^2 \rangle, \quad \gamma_B = \langle (\lambda_j^B)^2 \rangle. \quad (9)$$

Let us start to evaluate the corresponding ground-state energies per site for each of the above phases:

$$U_{O_1} = -\frac{15z|J|}{4} - \frac{9}{2}D_A - \frac{25}{8}D_B, \quad (10)$$

$$U_{O_2} = -\frac{10z|J|}{4} - 2D_A - \frac{25}{8}D_B, \quad (11)$$

$$U_{O_3} = -\frac{5z|J|}{4} - \frac{1}{2}D_A - \frac{25}{8}D_B, \quad (12)$$

$$U_{O_4} = -\frac{9z|J|}{4} - \frac{9}{2}D_A - \frac{9}{8}D_B, \quad (13)$$

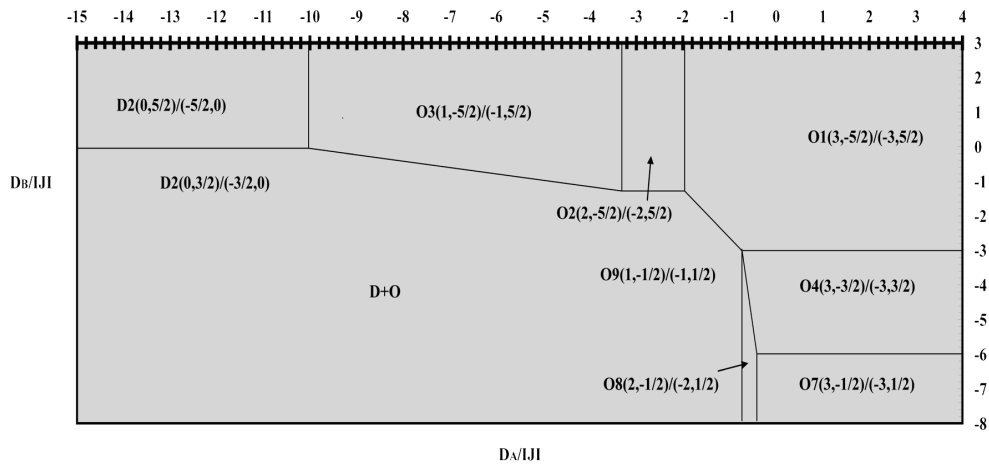


**Fig. 2.** Ground-state phase diagrams with the closest neighbor ( $z = 4$ ) and different crystal fields  $D_A$  and  $D_B$ . The ordered and disordered phases:  $O_1, O_2, O_3, O_4, O_7, O_8, O_9, D_1, D_2$ , and  $(D+O)$ :  $O_5, O_6, D_3$  are separated by thin lines, respectively

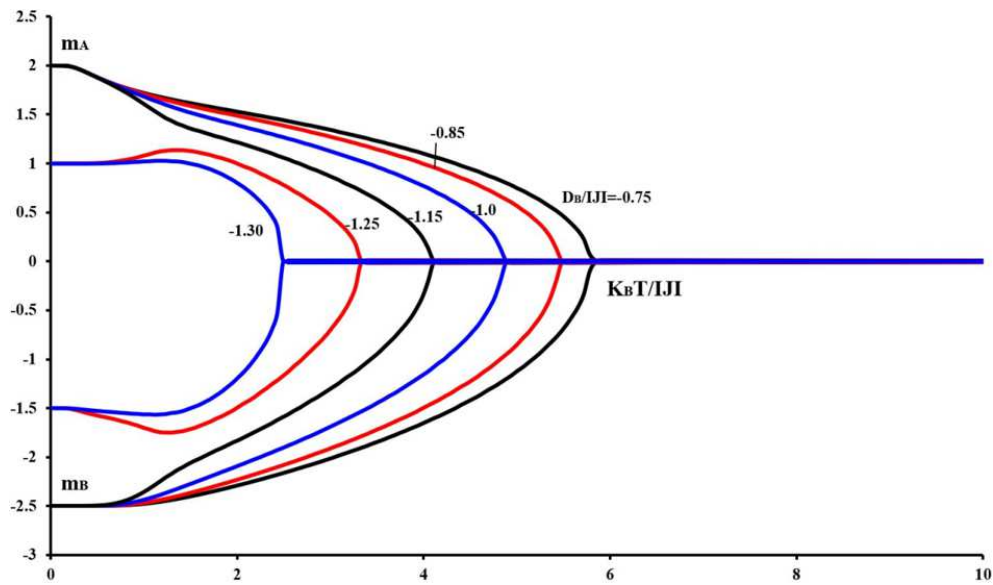


**Fig. 3.** Temperature dependences of the magnetizations of sublattices  $m_A, m_B$  for the white mixed ferrimagnet ( $z = 4$ ), when the value of  $D_B/|J|$  is changed, for fixed  $D_A/|J| = -3.0$

$$U_{O_5} = -\frac{6z|J|}{4} - 2D_A - \frac{9}{8}D_B, \quad (14) \quad U_{O_9} = -\frac{z|J|}{2} - D_A - \frac{1}{4}D_B, \quad (18)$$

$$U_{O_6} = -\frac{3z|J|}{4} - \frac{1}{2}D_A - \frac{9}{8}D_B, \quad (15) \quad U_{D_1} = -\frac{25}{8}D_B, \quad (19)$$

$$U_{O_7} = -\frac{3z|J|}{4} - \frac{9}{2}D_A - \frac{1}{8}D_B, \quad (16) \quad U_{D_2} = -\frac{9}{8}D_B, \quad (20)$$

$$U_{O_8} = -\frac{z|J|}{4} - \frac{1}{2}D_A - \frac{1}{8}D_B, \quad (17) \quad U_{D_3} = -\frac{1}{8}D_B. \quad (21)$$

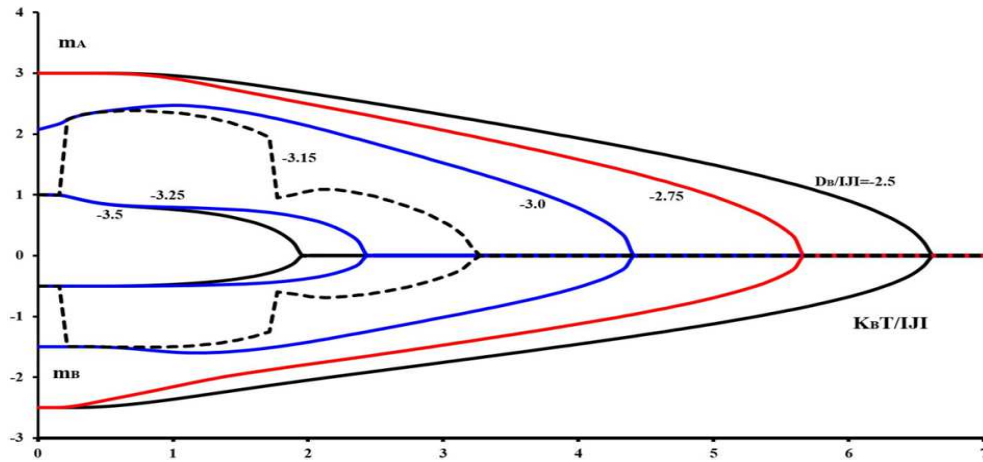


**Fig. 4.** Temperature dependences of the magnetizations of sublattices  $m_A$ ,  $m_B$  for the mixed ferrimagnet ( $z = 4$ ), when the value of  $D_B/|J|$  is changed, for fixed  $D_A/|J| = -1.25$

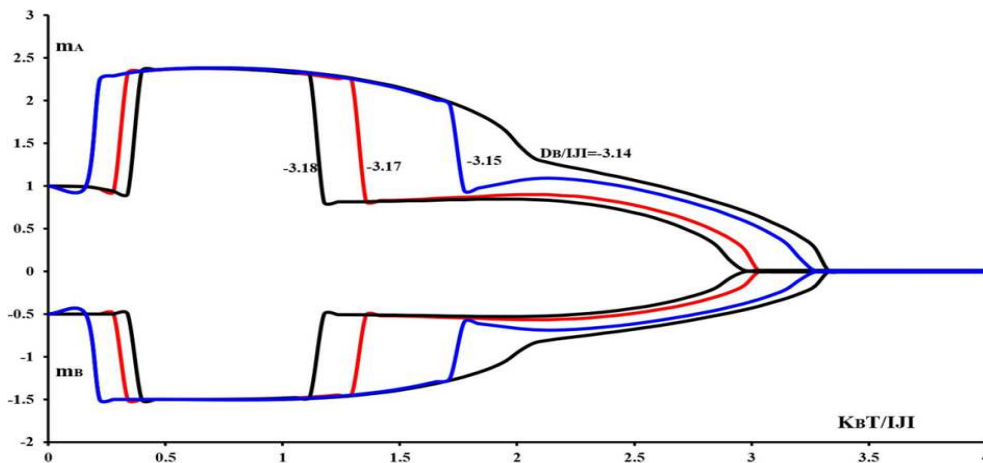


**Fig. 5.** Temperature dependences of the magnetizations of sublattices  $m_A$ ,  $m_B$  for the mixed-spin Ising ferrimagnet with the coordination number  $z = 4$ , when the value of  $D_B/|J|$  is changed, for fixed  $D_A/|J| = -1.25$

From the equations (i.e., Eqs. (10)–(21)), one can compare the energies to create the ground-state phase diagram of the system with  $z = 4$  as shown in Fig. 2.

#### 4. Magnetic Properties

From the ground-state phase diagram structure, one may find the thermal variation of the magnetizations of interpenetrated lattices  $m_A$  and  $m_B$ , solving numerically the coupled equations (5)–(7). For a square lattice, as  $D_B/|J|$  increases from  $D_B/|J| = -1.30$  to  $-0.75$ , for a constant value of  $D_A/|J|$ , the temperature dependence of  $m_A$  shows interesting features. So,

it is observed that phase transitions occur. In other words, within the range  $-1.30 < D_B/|J| \leq -0.75$ , the magnetizations of sublattices show distinguishable thermal variation behaviors, as illustrated in Fig. 3 [3, 17, 18]. It is worth to note that the proposed system is jumped at certain temperatures before being reached the transition temperature  $T_C$ , i.e., the magnetic system is passed through a first-order phase transition. Whereas, the sublattice magnetization is continuously altered that it does go to zero, because the configuration goes through two phases separating the ferrimagnetic or antiferromagnetic phase from the paramagnetic one. So, this phenomenon is defined as

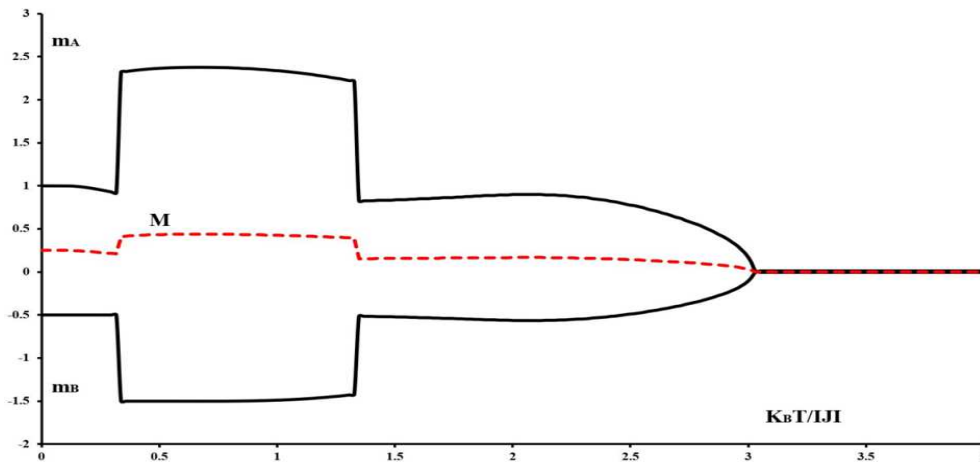


**Fig. 6.** A close view of thermal variations of the magnetizations of sublattices  $m_A$ ,  $m_B$  for the mixed-spin Ising ferrimagnet with the coordination number  $z = 4$ , when the value  $D_B/|J| = -3.17$ , for a fixed  $D_A/|J| = -1.25$

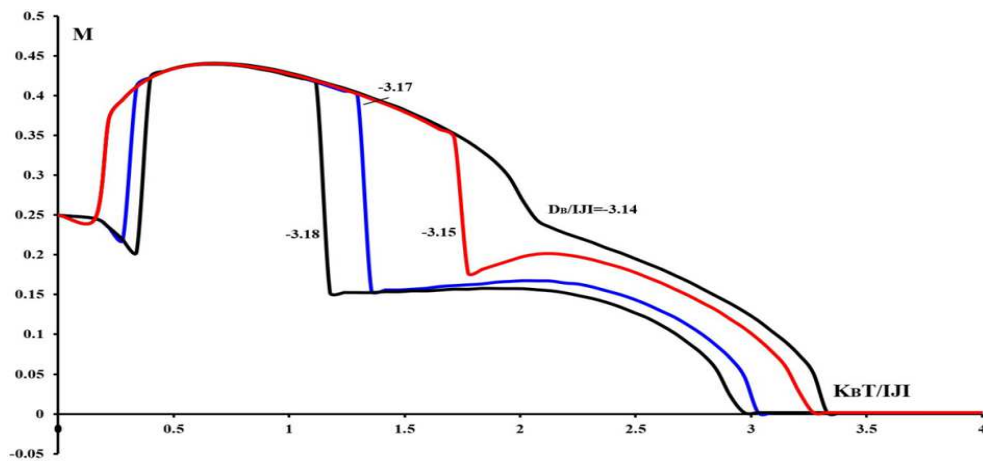


**Fig. 7.** Temperature dependences of the total magnetization  $M$  for the mixed-spin Ising ferrimagnet with the coordination number  $z = 4$ , when the value of  $D_B/|J|$  is changed, for fixed  $D_A/|J| = -1.25$

the second-order phase transition or the Curie transition [3, 17].

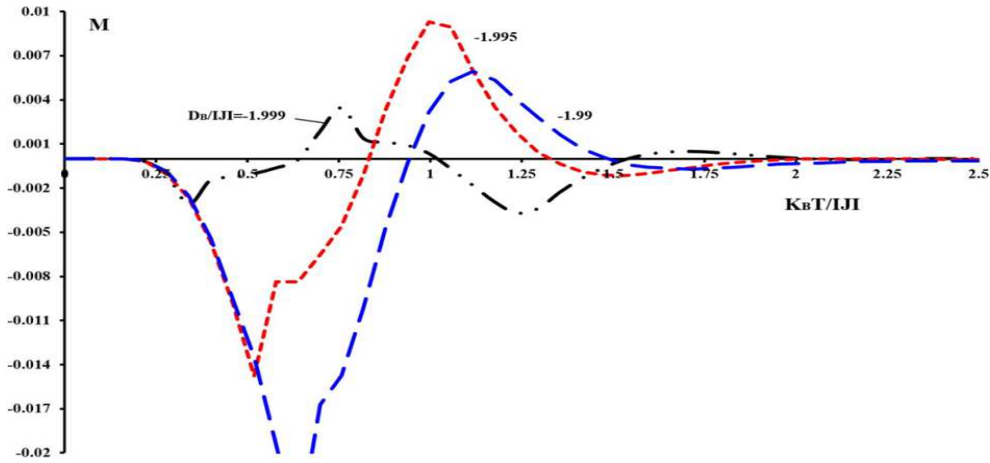
However, as  $D_B/|J|$  increases from  $D_B/|J| = -3.5$  to  $-2.5$  for a constant value of  $D_A/|J|$ , the temperature dependence of  $m_A$  shows interesting features. So, as is seen, a somewhat rapid decrease from its saturation magnetization occurs (Fig. 4).

Figure 5 exhibits distinctive features of the proposed system such as a re-entrant behavior, when the value of  $D_B/|J|$  is changed, for a fixed  $D_A/|J| = -1.25$ .

On the other hand, Figs. 5, 6, and 7, respectively, show clearly low-temperature phase diagrams in the

$(m_A, T)$ ,  $(m_B, T)$ , and  $(M, T)$  planes for the mixed-spin Blume–Capel ferrimagnet on a square lattice ( $z = 4$ ), in the region of  $-3.18 \leq D_B/|J| \leq -3.15$ , at  $D_A/|J| = -1.25$ , indicating the re-entrance phenomenon [3, 17, 27].

It is worth to note that the characteristic properties on a square lattice are examined. We found that a compensation temperature ( $T_k$ ) depends on the negative values of magnetic crystal fields, i.e.,  $-1.999 \leq D_B/|J| < -1.95$ . As shown in Fig. 8, the proposed system may exhibit interesting features in the global magnetization based on heat variations with a given value of  $D_A/|J| = -2.0$ , that



**Fig. 8.** Thermal variations of the total magnetization  $M$  for the mixed-spin Ising ferrimagnet with the coordination number  $z=4$ , when the value of  $D_B/|J|$  is changed, for fixed  $D_A/|J| = -2.0$

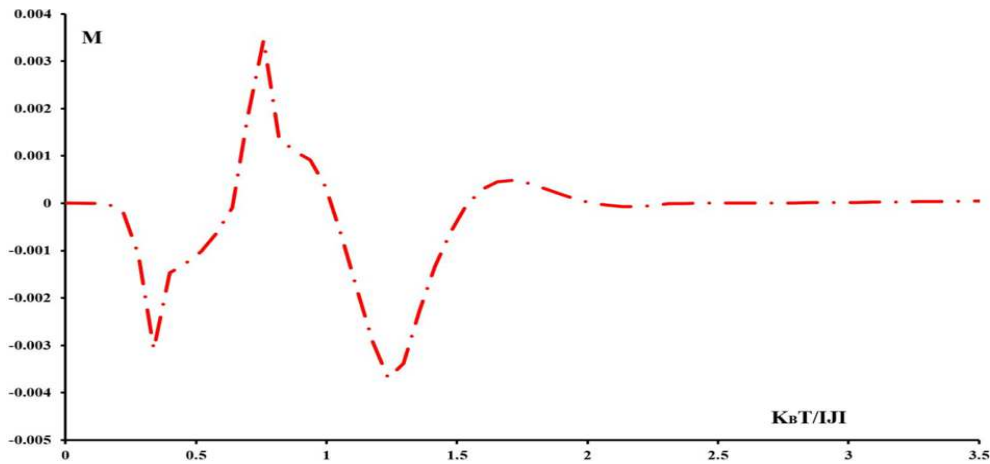


**Fig. 9.** A close view of the temperature dependences of the total magnetization for the mixed-spin Ising ferrimagnet with the coordination number  $z = 4$ , when  $D_A/|J| = -2.0$  and  $D_B/|J| = -1.999$

the system has three, four, or even five compensation temperatures for  $k_B T / |J| = 0$  and  $k_B T / |J| \neq 0$ , respectively. Figure 9 illustrates a close view the temperature dependences of the global magnetization. The system may have multiple compensation points.

As is seen from Figs. 8 and 9, in the region, where the system may show a compensation point, the spin-3 sublattice is more ordered than the spin-5/2 sublattice below the compensation temperature. The sublattice magnetization undergoes to be cancelled, but it is still incomplete. So there is a spontaneous magnetization remaining in the system (i.e.,  $M \neq 0$ ). This is the evidence of the antiferromagnetic near neigh-

bor interactions. As the system temperature is increased, the direction of this residual magnetization can switch because of the thermal excitation. The compensation behaviors shown in Figs. 8 and 9 indicate the crossing points between the magnitudes of  $m_A$  and  $m_B$  which prove the eligibility of Eqs. (5) and (6), respectively [3, 25]. It is worth mentioning that the molecular MFT in the ferrimagnetic case predicts the presence of a compensation point in the ordered phase, where the total moment vanishes [3, 9].

We have investigated the impact of the free energy on the thermodynamic phase steadiness of the proposed system. The free energy of the present

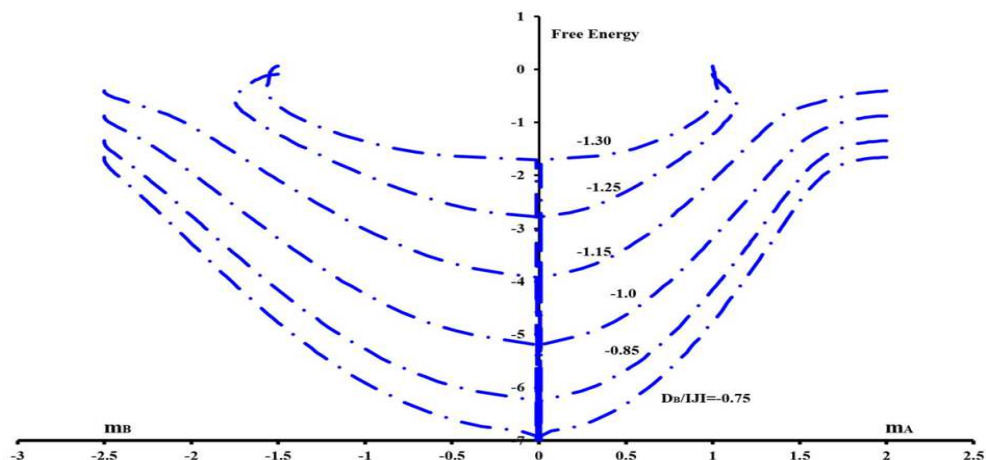


**Fig. 10.** Free energy variations with the magnetizations of sublattices for a  $z = 4$  of the mixed-spin ferrimagnet for various values of  $D_B/|J|$ , when the magnitude of  $D_A/|J| = -3.0$

system has been calculated according to Eq. (4);, so, the system behaviors are illustrated in Fig. 10, on a square lattice. The behavior of a ferrimagnetic or antiferromagnetic state (at a compensation point  $T < T_C$ ) and paramagnetic one (at transition temperature  $T > T_C$ ) is based on the curve of free energy that exhibits an inflexion that correlates to a discontinuity. However, at a critical anisotropy value, the free energy of the system is continuous [25, 31]. As a result, the magnetization curves constantly decrease to zero, separating the ferrimagnetic phase from the paramagnetic phase; this occurrence is termed as a phase transition of the second-order or the Curie point. When the magnetization falls to zero or some value, a first-order phase transition happens, or, perhaps, the temperature at which the magnetization leap occurs [25, 27].

## 5. Conclusions

the molecular mean-field approximation (MMFA) is used on the basis of Bogoliubov inequality for the free energy. A ground-state phase diagram of the mixed spin-3 and spin-5/2 Blume–Capel Ising ferrimagnetic system is analyzed with different crystal field domains, i.e., magnetic anisotropies have been constructed. A compensation point exists or doesn't for a such system which has not yet been investigated. The magnetic properties of the proposed lattice have been evaluated to solve the general expressions numerically. In this respect, the character-

istic features of the magnetization curves may express a spin compensation phenomenon (one can observe Figs. 8 and 9, respectively). One may compare the obtained results with those of a system with mixed spin-2 and spin-5/2 on a square lattice [12]. The researchers presented a ground-state phase diagram and examined the ferrimagnetic properties of the model. On the other hand, a theoretical study dealing with the mixed spin-2 and spin-3/2 Ising model was treated using mean-field theory [25]. So, it has been determined phase diagrams of the considered system. The authors obtained multicritical points and reentrant behavior, when the spin crystal fields, i.e., anisotropies  $D_A/|J|$   $D_B/|J|$  acting on both ions increase. However, the present system may display five compensation points. In addition, we report on new magnetic re-entrant behaviors with the phase (1, -0.5) for various values of crystalline anisotropies acting on B-ions (observe Fig. 5). It is demonstrated that a decrease in the magnetic anisotropy of B-atoms causes a decrease in the transition temperature (see Figs. 3, 4, and 5, respectively). The recent results may be useful for supporting the magnetic properties of a series of molecular-based magnets. It is worth to note that R–Mn links are large enough just to recover and realign the manganese moments of the Mn–R–Mn slabs. This gives rise to the ferromagnetic structures of Nd- and SmMn<sub>6</sub>Ge<sub>6</sub> and the antiferromagnetic exchange interaction observed in RMn<sub>6</sub>Sn<sub>6</sub> complexes, respectively [10, 11].

1. S.K. Ghatak. Magnetic behaviour of a disordered Ising ferrimagnet in a high magnetic field. *Philosophical Magazine* **92** (1–3), 120 (2011).
2. S. Ohkoshi, Y. Abe, A. Fujishima, K. Hashimoto. Design and preparation of a novel magnet exhibiting two compensation temperatures based on molecular field theory. *Phys. Rev. Lett.* **82**, 1285 (1999).
3. O.F. Abubrig, D. Horvath, A. Bobak, M. Jascur. Mean-field solution of the mixed spin-1 and spin-3/2 Ising system with different single-ion anisotropies. *Phys. A* **296**, 437 (2001).
4. A. Jabar, R. Masrouf, A. Benyoussef, M. Hamedoun. Magnetic properties of the mixed spin-1 and spin-3/2 Ising system on a bilayer square lattice: A Monte Carlo study. *Chem. Phys. Lett.* **670**, 16 (2017).
5. J. Kplé, S. Massou, F. Hontinfinde, E. Albayrak. Spin-1/2 Ising model on a AFM/FM two-layer Bethe lattice in a staggered magnetic field. *Chinese J. Phys.* **56** 1252 (2018).
6. W. Linert, M. Verdaguer. *Molecular Magnets, Recent Highlights* (Springer, 2003).
7. D. Gatteschi. Molecular Magnetism: A basis for new materials. *Adv. Mater.* **6**, 635 (1994).
8. J.S. Miller, A.J. Epstein. Designer Magnets. *Chem. Eng. News* **73** (40), 30 (1995).
9. T. Kaneyoshi, E.F. Sarmiento, I.P. Fittipaldi. A Compensation temperature induced by transverse fields in a mixed ising ferrimagnetic system. *Jpn. J. Appl. Phys.* **27** (4), L690 (1988).
10. J.H.V.J. Brabers, V.H.M. Duijn, F.R. de Boer. Magnetic properties of rare-earth manganese compounds of the RMn<sub>6</sub>Ge<sub>6</sub> type. *J. Alloys and Compounds* **198**, 127 (1993).
11. G. Venturini, B. Chafik, El. Idrissi, E. Ressouche, B. Malaman. Magnetic structure of YbMn<sub>6</sub>Ge<sub>6</sub> from neutron diffraction study. *J. Alloys and Compounds* **216**, 243 (1995).
12. C.A. Mercado, N. De La Espriella, L.C. Sánchez. Ground state phase diagrams for the mixed Ising 2 and 5/2 spin model. *J. Magn. Magn. Mater.* **382**, 288 (2015).
13. M. Karimou, R.A. Yessoufou, G.D. Ngantso, F. Hontinfinde, A. Benyoussef. Mean-field and Monte Carlo studies of the magnetic properties of a spin-7/2 and spin-5/2 Ising bilayer film. *J. Supercond. Nov. Magn.* **32**, 1769 (2018).
14. M. Jašnišur, T. Kaneyoshi. The effect of anisotropies on the transition temperature in a spin-1/2 and spin-3/2 bilayer system with disordered interfaces. *Phys. A Stat. Mech. its Appl.* **220** (3–4), 542 (1995).
15. T. Kaneyoshi, M. Jascur. Magnetic properties of a ferromagnetic or ferrimagnetic bilayer system. *Physica A* **195**, 474 (1993).
16. A. Bobàk. The effect of anisotropies on the magnetic properties of a mixed spin-1 and spin-3/2 Ising ferrimagnetic system. *Phys. A* **258**, 140 (1998).
17. T. Kaneyoshi, Y. Nakamura, S. Shin. A diluted mixed spin-2 and spin-5/2 ferrimagnetic Ising system; A study of a molecular-based magnet. *J. Phys.: Condens. Matter* **10**, 7025 (1998).
18. Y. Nakamura. Existence of a compensation temperature of a mixed spin-2 and spin-5/2 Ising ferrimagnetic system on a layered honeycomb lattice. *Phys. Rev. B* **62** (17), 11742 (2000).
19. A. Ozkan. A simulation of the mixed spin 3-spin 3/2 ferrimagnetic Ising model. *Phase Transitions; A Multinational J.* **89** (1), 94 (2015).
20. M. Godoy, V.S. Leite, W. Figueiredo. Mixed-spin Ising model and compensation temperature. *Phys. Rev. B* **69**, 054428 (2004).
21. R. Masrouf, A. Jabar, L. Bahmad, M. Hamedoun, A. Benyoussef. Magnetic properties of mixed integer and half integer spins in a Blume–Capel model: A Monte Carlo study. *J. Magn. Magn. Mater.* **421**, 76 (2017).
22. R. Masrouf, A. Jabar. Magnetic properties of multilayered with alternating magnetic wires with the mixed spins-2 and 5/2 ferrimagnetic Ising model. *Superlattices and Microstructures* **109**, 641 (2017).
23. B. Deviren, M. Keskin, O. Canko. Magnetic properties of an anti-ferromagnetic and ferrimagnetic mixedspin-1/2 and spin-5/2 Ising model in the longitudinal magnetic field within the effective-field approximation. *Physica A* **388**, 1835 (2009).
24. A. Dakhama, N. Benayad. On the existence of compensation temperature in 2d mixed-spin Ising ferrimagnets: an exactly solvable model. *J. Magn. Magn. Mater.* **213**, 117 (2000).
25. H. Miao, G. Wei, J. Geng. Phase transitions and multicritical points in the mixed spin-3/2 and spin-2 Ising model with different single-ion anisotropies. *J. Magn. Magn. Mater.* **321**, 4139 (2009).
26. G.M. Buendia, J.A. Liendo. Monte Carlo simulation of a mixed spin 2 and spin Ising ferrimagnetic system. *J. Phys.: Condens. Matter* **9**, 5439 (1997).
27. E. Albayrak, A. Yigit. Mixed spin-3/2 and spin-5/2 Ising system on the Bethe lattice. *Phys. Lett. A* **353**, 121 (2006).
28. J.Oitmaa, I.G. Enting. A series study of a mixed-spin  $S = (\frac{1}{2}, 1)$  ferrimagnetic Ising model. *J. Phys.: Condens. Matter* **18**, 10931 (2006).
29. P.J.B. Clarricoats, H.M. Barlow. *Microwave Ferrites* (Chapman & Hall, cop. Un. College, 1961).
30. L. Neel. Magnetic properties of ferrites: ferrimagnetism and antiferromagnetism. *Annls. Phys.* **3**, 137 (1948).
31. S. Ferlay, T. Mallah, R. Ouahès, P. Veillet, M. Verdaguer. A room- temperature organometallic magnet based on Prussian blue. *Nature* **378**, 701 (1995).

Received 13.05.22

*I.A. Обейд, Х.К. Мохамад, Ш.Д. Аль-Саїді*

ХАРАКТЕРИСТИКИ ФЕРИМАГНЕТИКА  
І ТЕМПЕРАТУРИ КОМПЕНСАЦІЇ СПІНІВ  
В МОДЕЛІ БЛУМ–КАПЕЛЯ  
ЗІ ЗМІШАНИМИ СПІНАМИ З ТА 5/2

Розглянуто теорію молекулярного середнього поля з використанням функції Гіббса–Боголюбова для вільної енергії феримагнетика зі спінами 3 та 5/2 для різних полів у магнітному кристалі в моделі Блум–Капеля. Оцінено значення вільної енергії, що залежить від вибору оператора Гамільтона. Мінімізуючи вільну енергію даної системи, ми отри-

мали характеристики поздовжньої магнетизації, температур компенсації та оборотної поведінки при низьких температурах. Ми розглядаємо вплив магнітної анізотропії на критичні явища і обговорюємо залежність вільної енергії від магнетизації підґратки. Наші результати передбачають існування кратних точок компенсації спінів в розупорядкованій системі Блум–Капеля для квадратної ґратки.

*Ключові слова:* модель Блум–Капеля зі змішаними спінами, поле магнітного кристала, фазові переходи, оборотна поведінка, температура компенсації спінів.